NOVEMBER 18TH, NAATBATT INTERNATIONAL

SODIUM ZINC BATTERY WORKSHOP, LOS ANGELES, CALIFORNIA

How Does an Antisolvent Additive Affect All Interfaces In Aqueous Zn–MnO_2 Batteries?

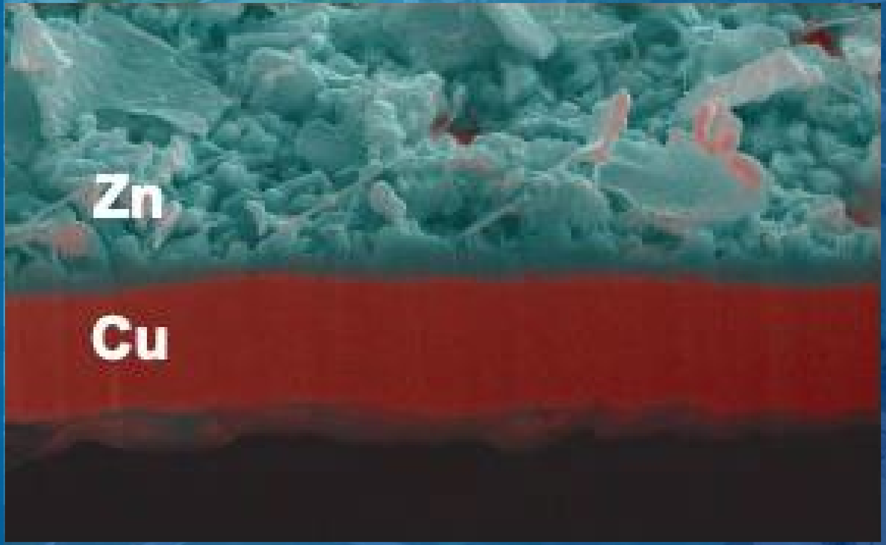

SANJA TEPAVCEVIC
Chemist
Materials Science Division

U.S. DEPARTMENT of ENERGY
Argonne National Laboratory is a U.S. Department of Energy laboratory managed by UChicago Argonne, LLC.

Argonne NATIONAL LABORATORY

ADDITIVES IN NEUTRAL pH Zn BATTERIES

Controlling Zn^{2+} solvation for uniform zinc plating and minimizing corrosion

ZHS: $Zn_4(OH)_6SO_4 \cdot n\ H_2O$

Insulating side product from hydrogen evolution and zinc corrosion

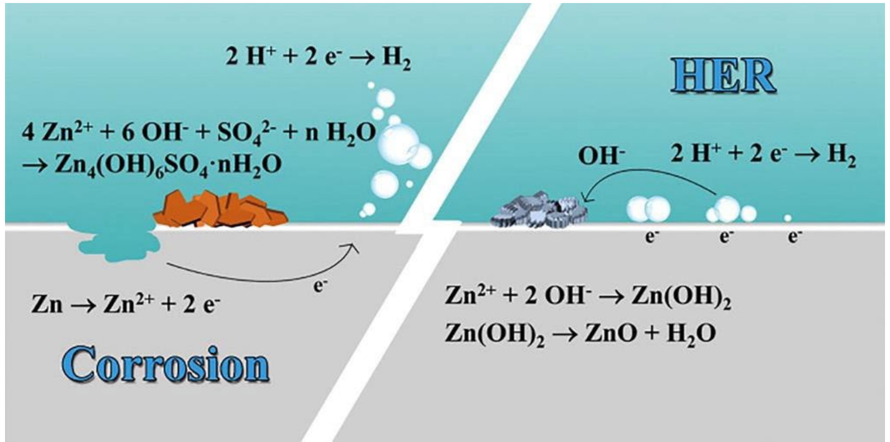

10.1016/j.jechem.2021.04.016

- Water-in-Salt

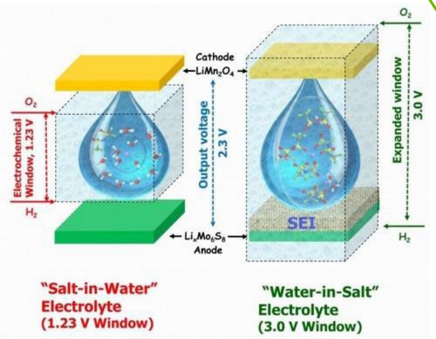

10.1126/science.aab1595

20m 10m 5m

10.1038/s41563-018-0063-z

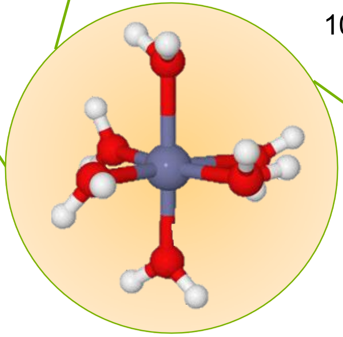

$[Zn(H_2O)_6]^{2+}$

- Chelating Agents

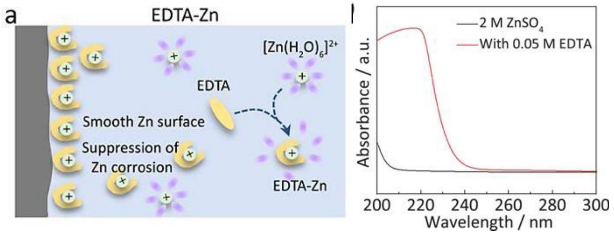

10.1002/adma.202200677

- Organic Solvents

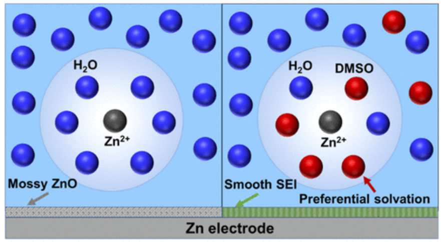

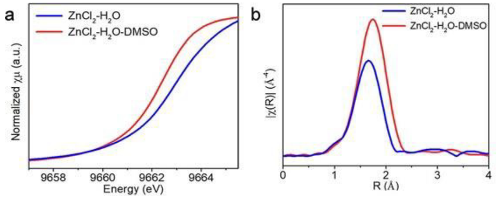

10.1021/jacs.0c09794

CO-SOLVENTS VS. ANTI-SOLVENTS

Can the Zn^{2+} solvation shell be influenced with something other than H_2O?

Co-Solvent

Both solvents can dissolve the salt in the electrolyte

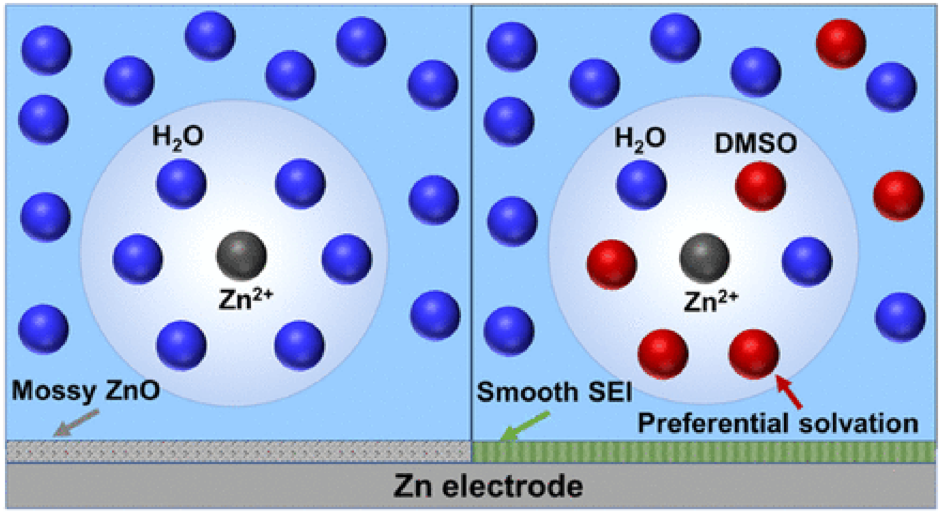

10.1021/jacs.0c09794

Anti-Solvent

The additive is soluble in the first solvent but does not dissolve the salt

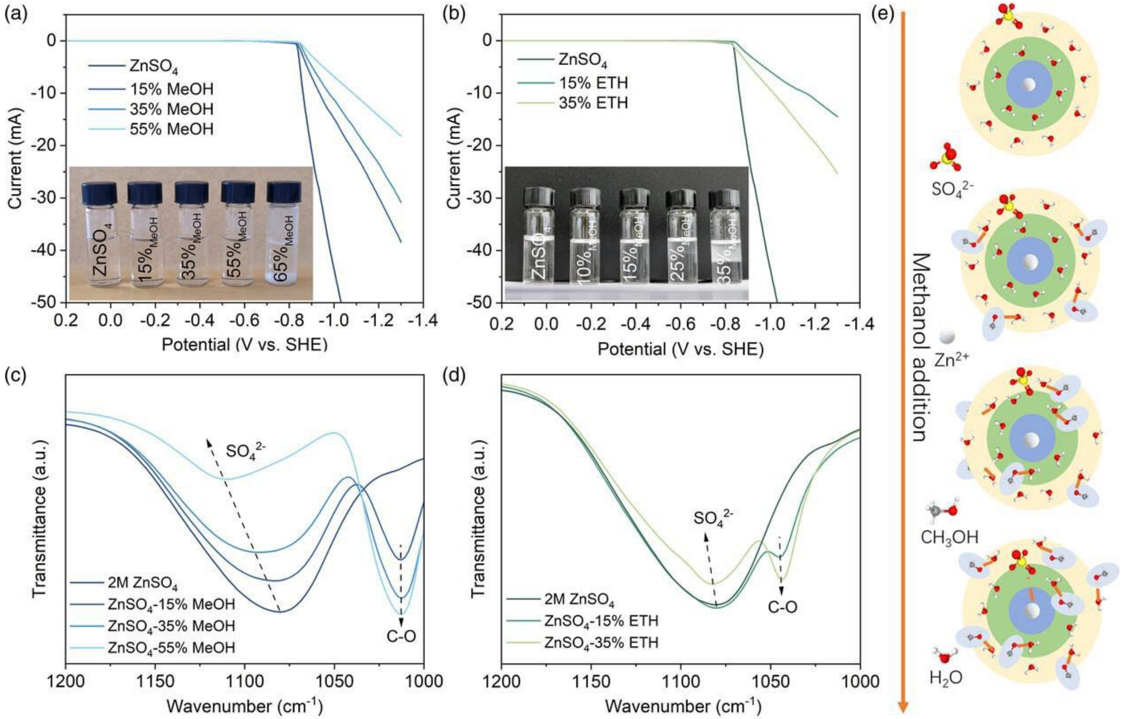

10.1002/sstr.202200270

ACETONITRILE WITH ZINC SULFATE AND WATER

Many studies over-exaggerate or don’t interrogate the additive’s ability to solvate Zn^{2+}

Computational prediction of Zn-H_2O-ACN complexes in bulk solution

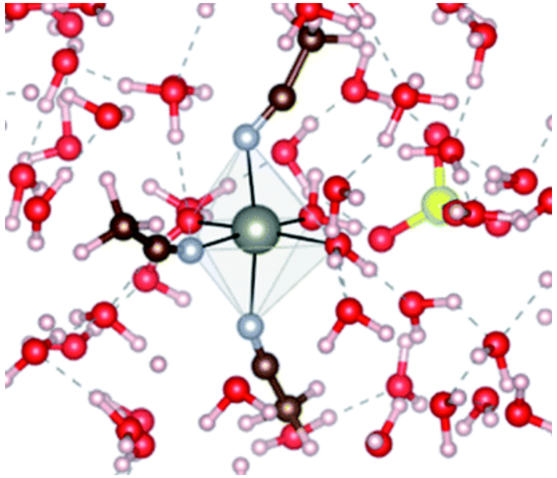

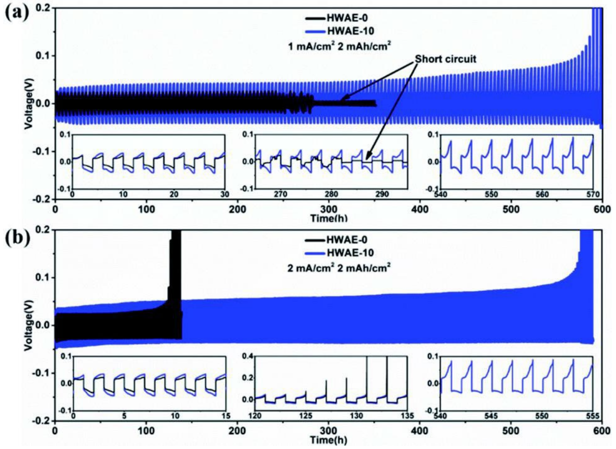

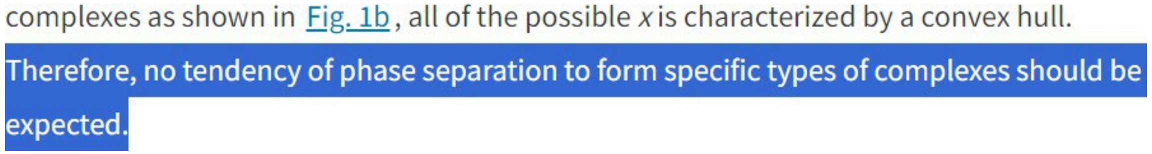

complexes as shown in Fig. 1b, all of the possible *x* is characterized by a convex hull. Therefore, no tendency of phase separation to form specific types of complexes should be expected.

10.1039/D0TA06622B

Phase separation of ZnSO4 solutions shows inability to solvate

ACN-rich top phase

Zn-rich bottom phase

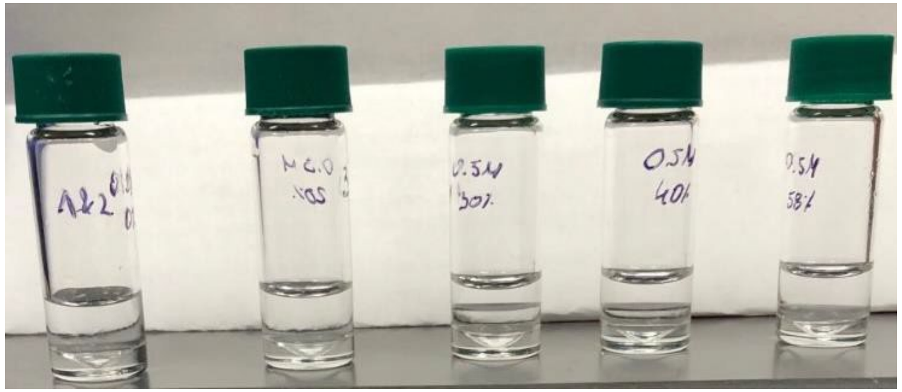

Stefan Ilic, Michael J. Counihan, Sydney N. Lavan, Yingjie Yang, Yinke Jiang, Diwash Dhakal, Julian Mars, Emma N. Antonio, Luis Kitsu Iglesias, Timothy T. Fister, Yong Zhang, Edward J. Maginn, Michael F. Toney, Robert F. Klie, Justin G. Connell, and Sanja Tepavcevic *Effect of Antisolvent Additives in Aqueous Zinc Sulfate Electrolytes for Zinc Metal Anodes: The Case of Acetonitrile*, *ACS Energy Letters* 2024 *9* (1), 201-208. doi: 10.1021/acsenergylett.3c02504

Counihan, M. J., Roberts, L., Ilic, S., Yang, Y., Ely, C., Klie, R. F., Toney, M. F., & Tepavcevic, S. How does an antisolvent additive affect all interfaces in aqueous Zn–MnO2 batteries?. Journal of Materials Chemistry A, 13(23), 17730-17739. (2025). doi:10.1039/D5TA00951K.

Neelam Omprakash Sunariwal, Thanh Le, Xiaoran Yang, Trenton Gallagher, Jordi Cabana, Tim Vosburgh and Sanja Tepavcevic *Effect of Pre-Conditioning on Cycling Performance of Aqueous Zn-Ion Batteries* (submitted)

BULK SOLVATION

X-ray studies and Raman spectroscopy conclusively show ACN is *NOT* in the first solvation shell of Zn^{2+}, no matter the concentration

XANES

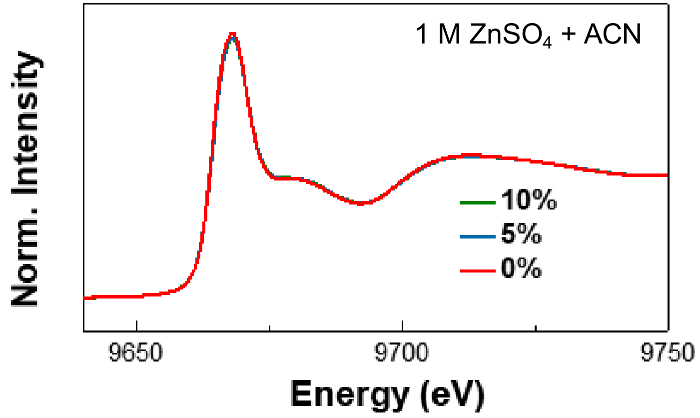

EXAFS

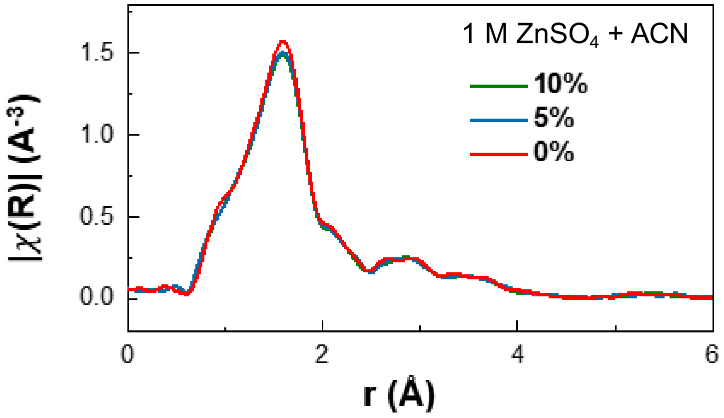

PDF

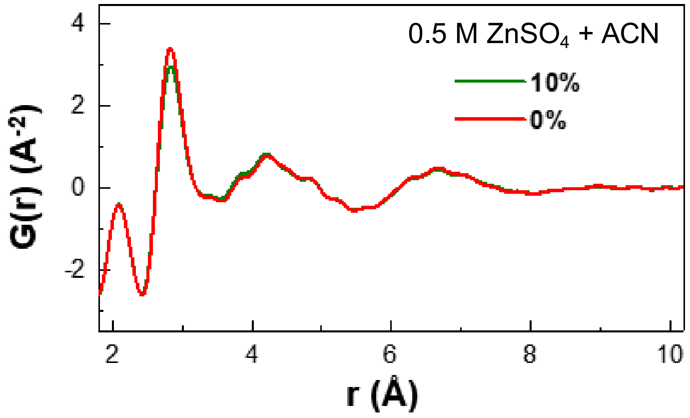

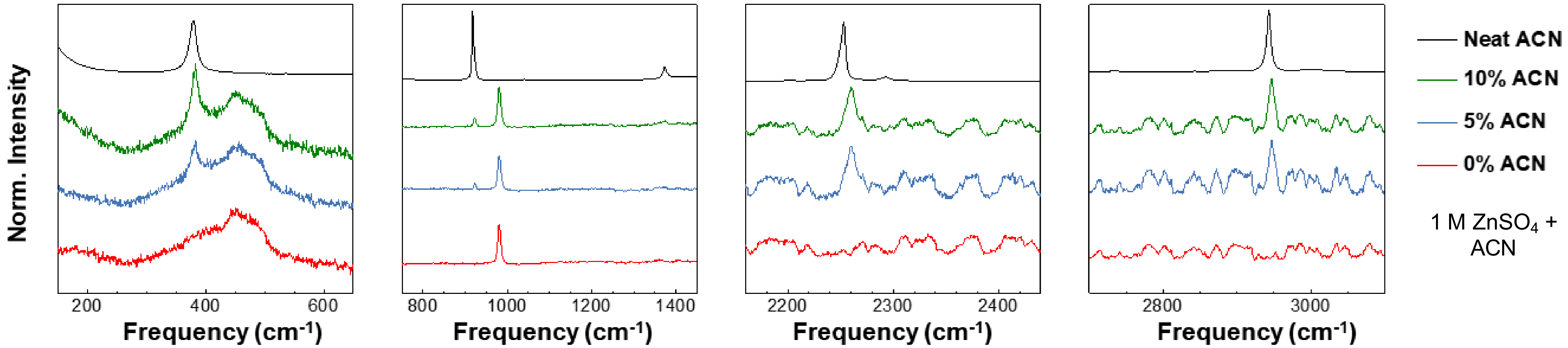

XAS courtesy of Diwash Dhakal
PDF courtesy of Dr. Julian Mars / Dr. Emma Antonio

INTERFACIAL SOLVATION: DOUBLE LAYER

Capacitance measurements show an increase in C_{dl} with increasing ACN, pointing to changes in double layer structure

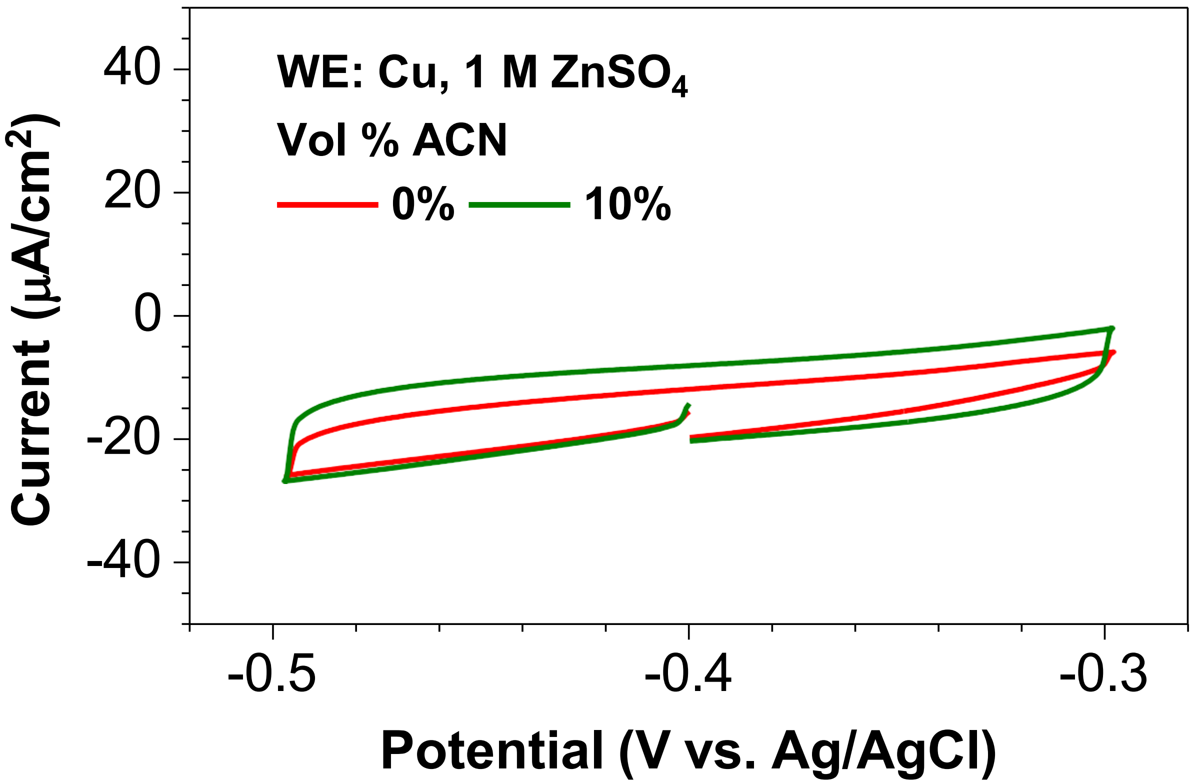

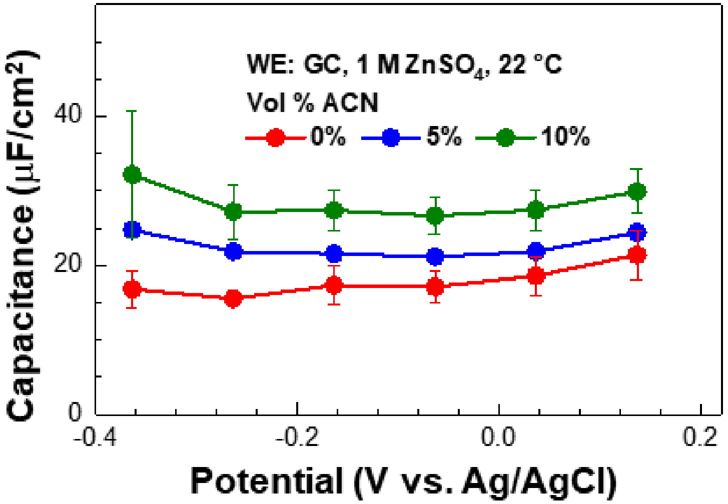

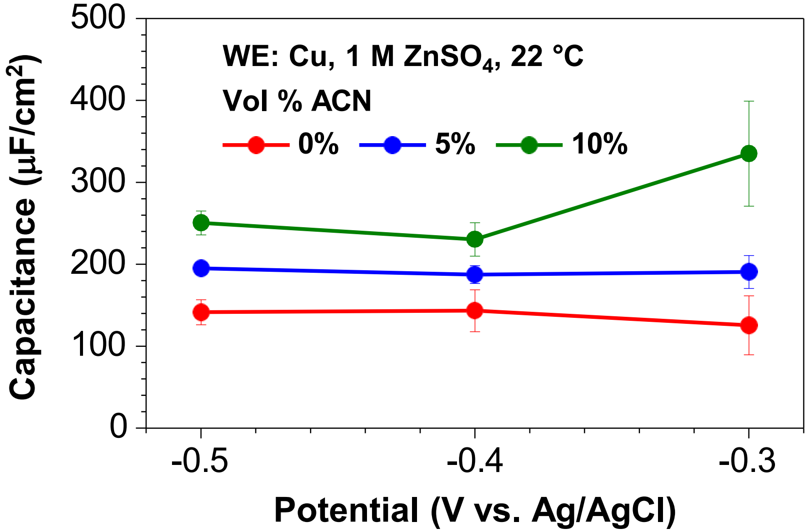

INTERFACIAL SOLVATION: SHINERS

Surface-enhanced Raman spectroscopy shows subtle shifts in ACN signal depending on the electrode chemistry and potential

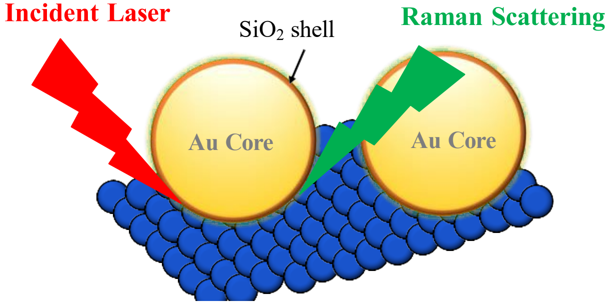

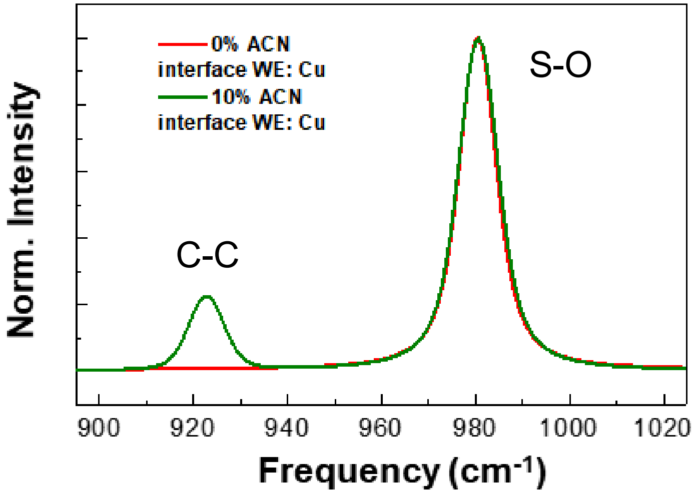

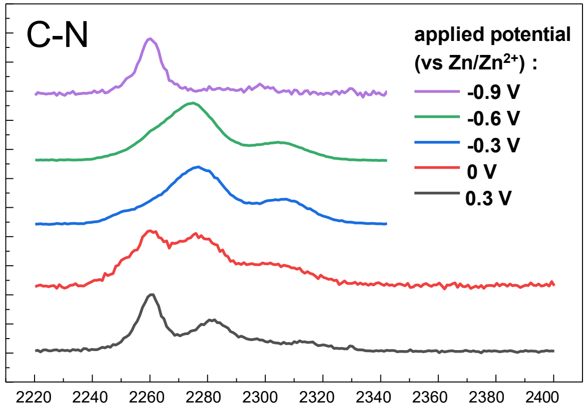

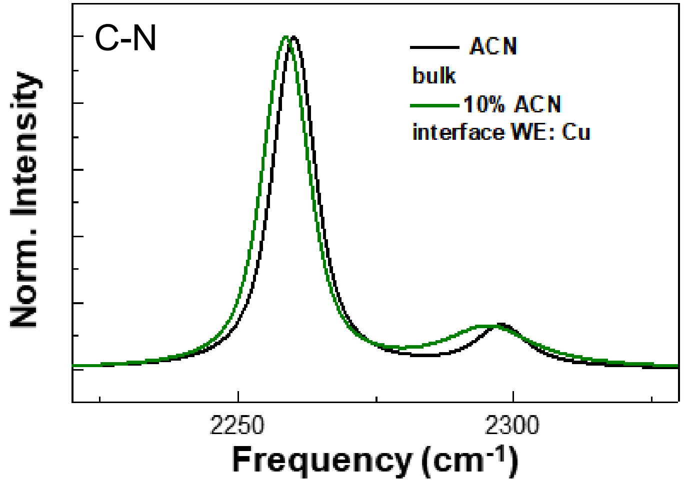

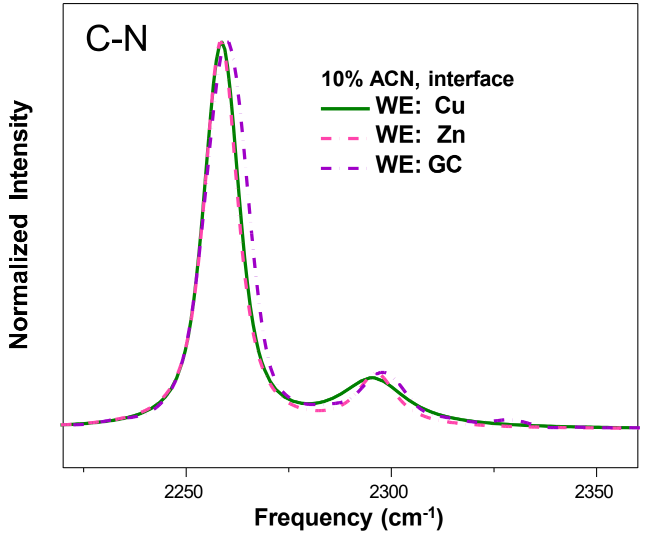

SHINERS courtesy of Dr. Sydney Lavan

INTERFACIAL SOLVATION: SIDE REACTIONS

Electrochemical hydrogen evolution reaction (HER) is suppressed with ACN, and invariance with cation valence shows interface over bulk effect

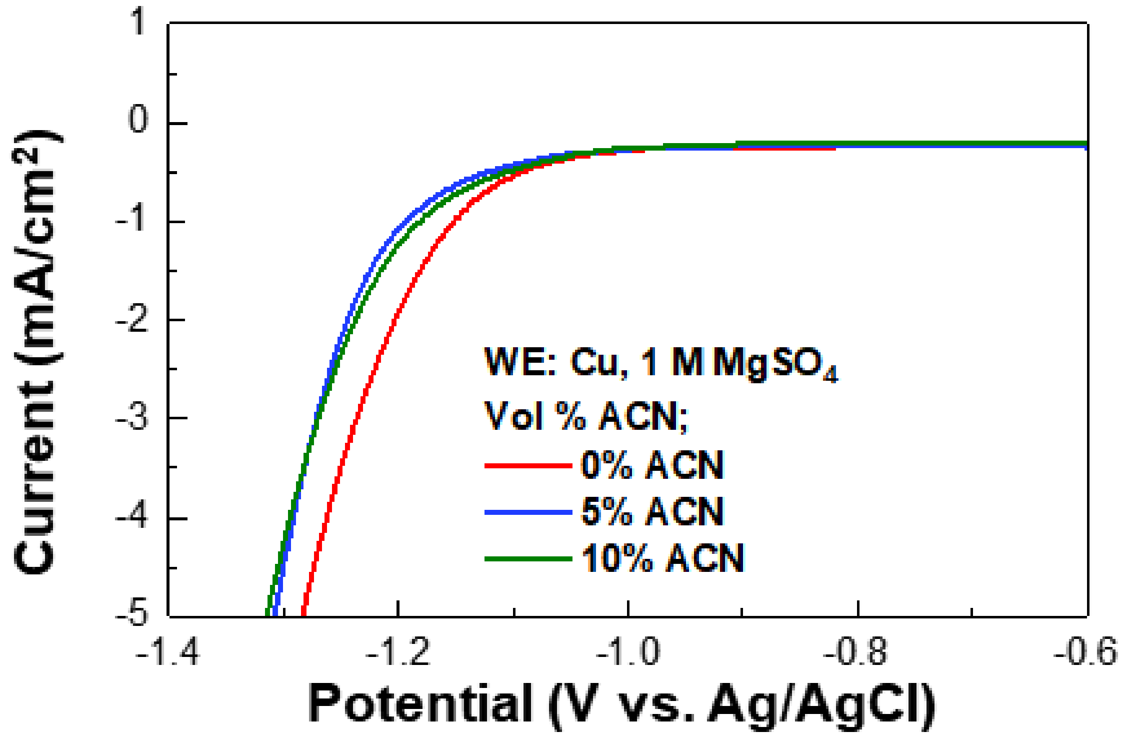

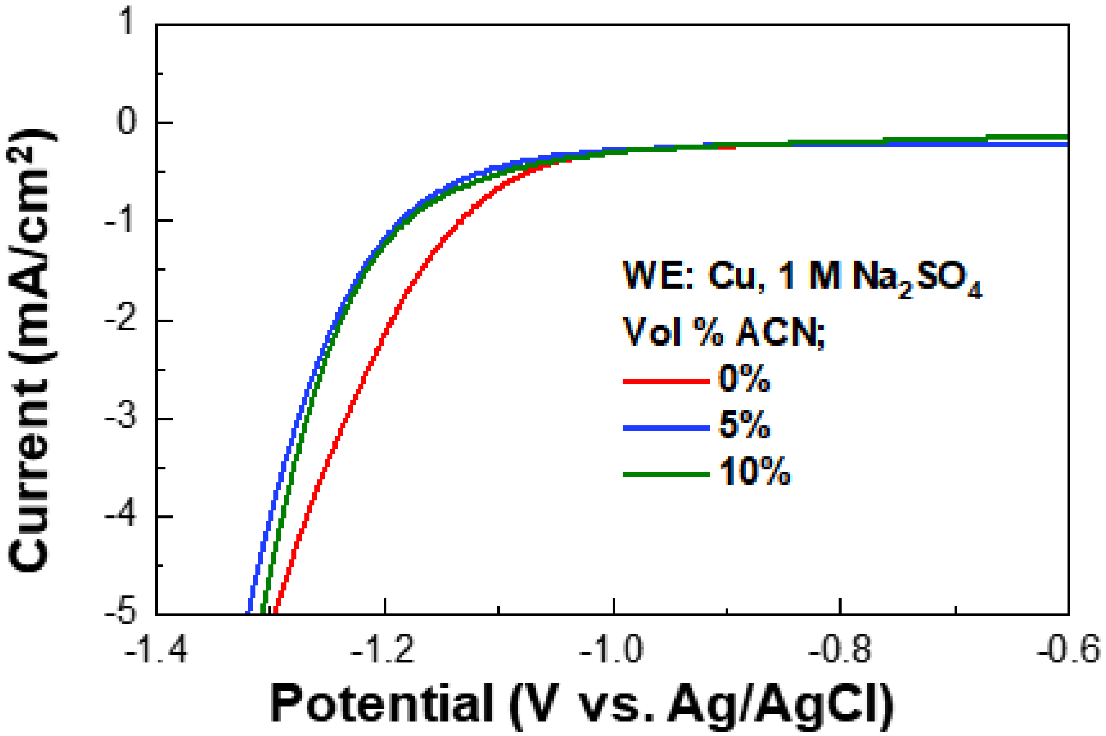

ZINC PLATING: OVERPOTENTIAL

Charge transfer overpotential increases with 5 and 10 vol % ACN, apparent in voltammetry and half cells with various electrodes

~30 mV increase in overpotentials

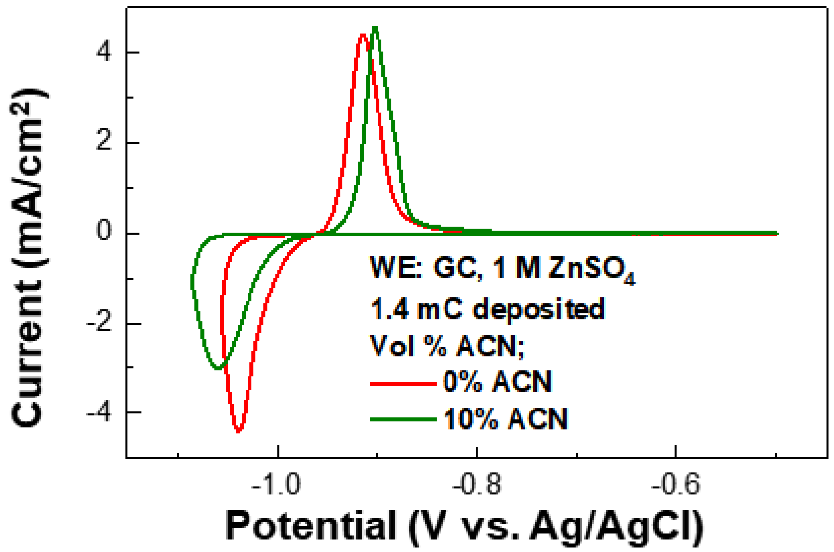

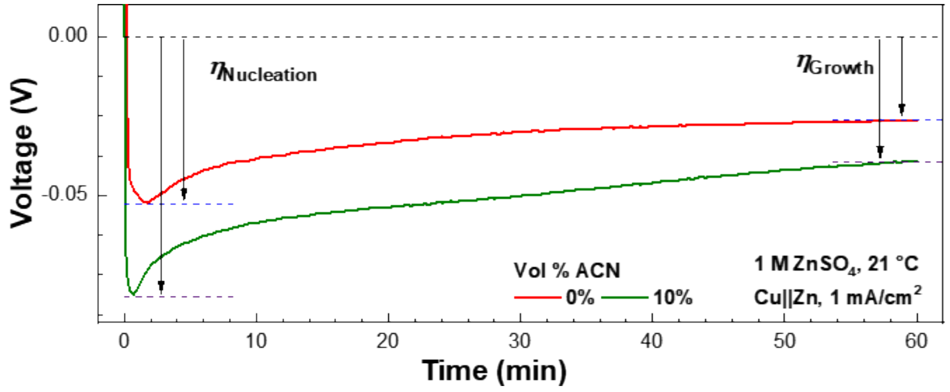

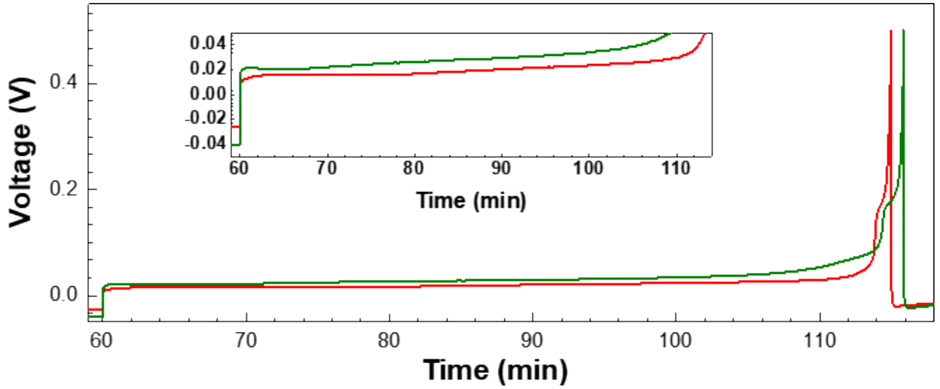

ZINC PLATING: INITIAL MORPHOLOGY

Adding ACN decreases initial Zn nuclei size and marginally more compact deposits compared to pure aqueous solution

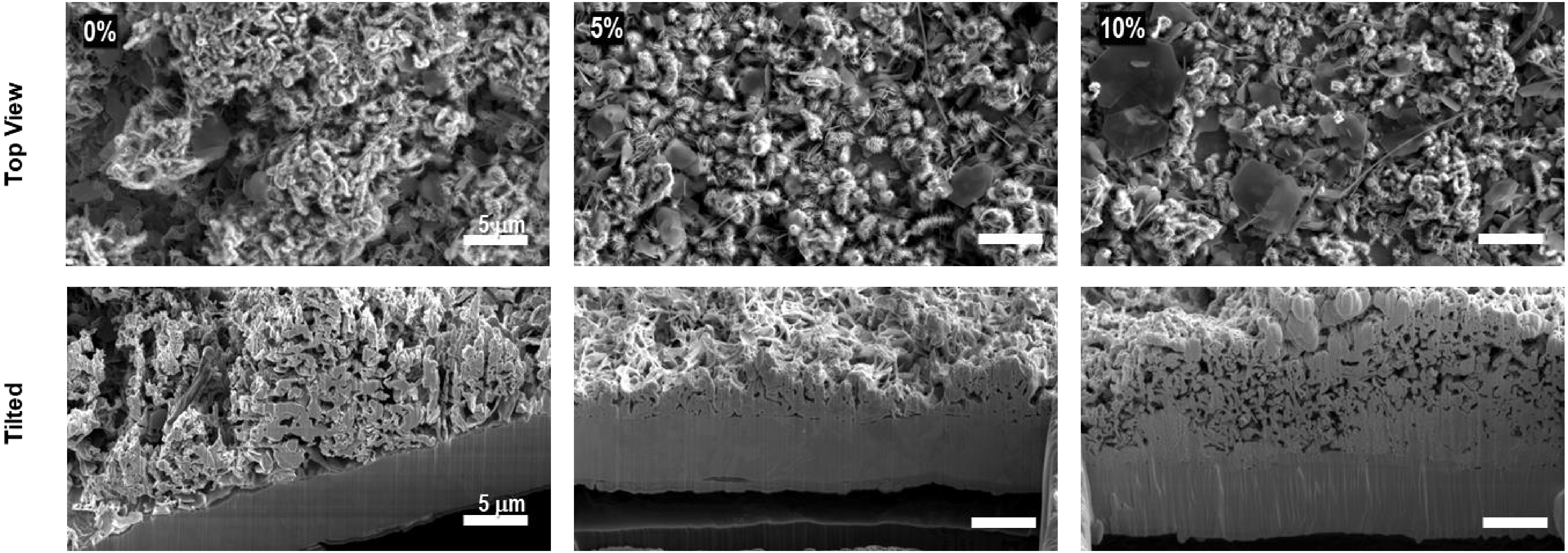

PFIB-SEM/EDX courtesy of Dr. Yingjie Yang

ELECTRODE EFFECTS: ALLOYING

Preliminary X-ray diffraction results show alloy compositions of Cu_4Zn_1, possibly up to Cu_5Zn_8

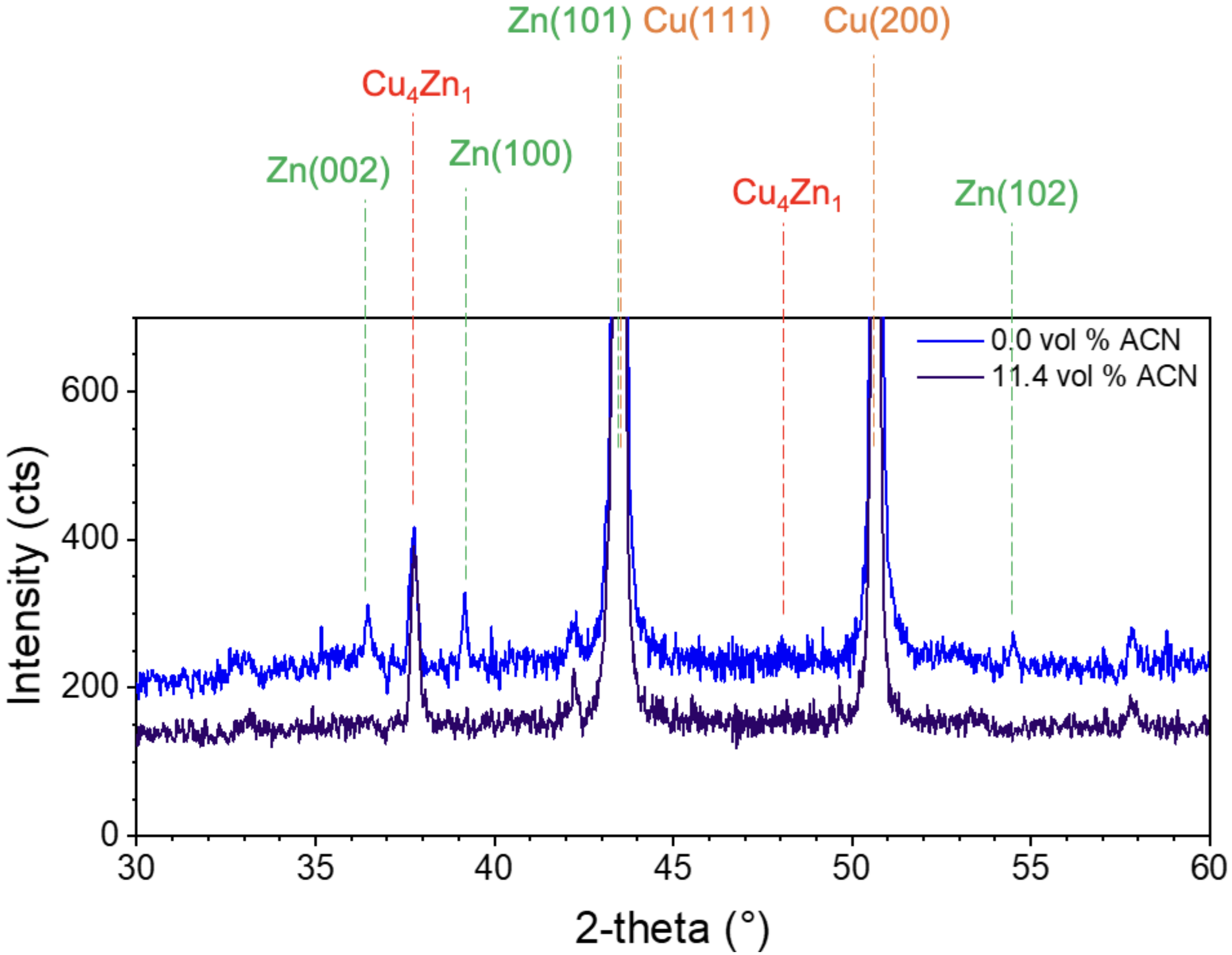

ONSET CHARGE AT LOWER CURRENT

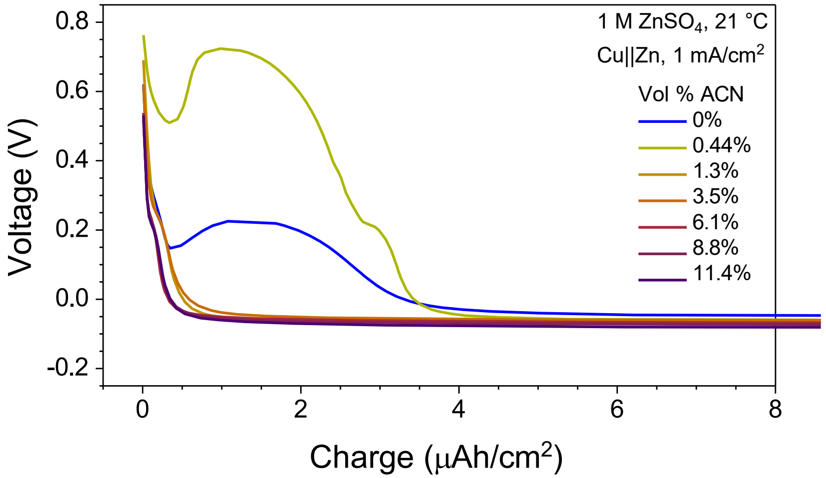

- **Alloying and UPD with Cu electrode is dependent on ACN, especially at low concentration**
- Peak in “non-Zn^0” charges in the 0.50-0.75-1.00 vol % ACN range
- One monolayer of UPD Zn@Cu is about 0.34 mC/cm^2
- 3 μAh/cm^2 ~ 10 mC/cm^2 ~ 30 monolayers
- Thin metal layer can promote uniform and stable metal growth

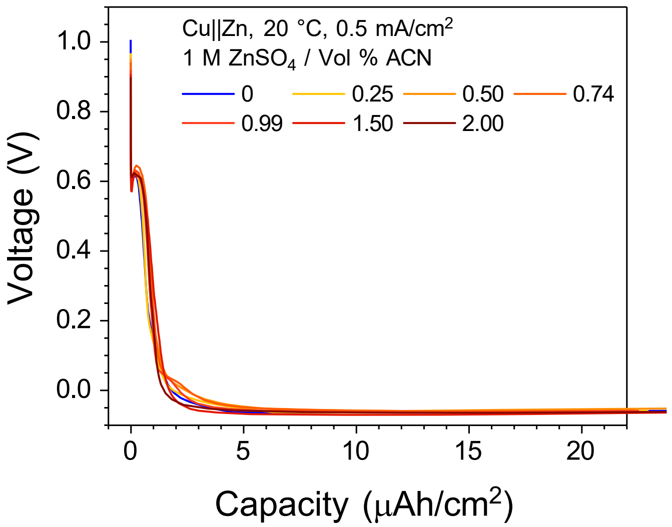

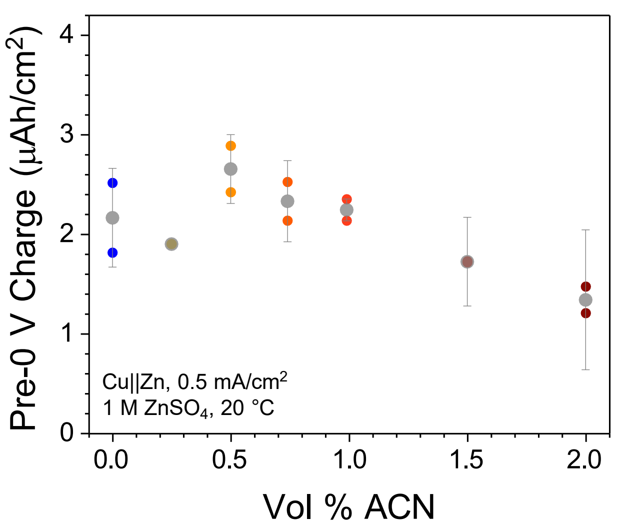

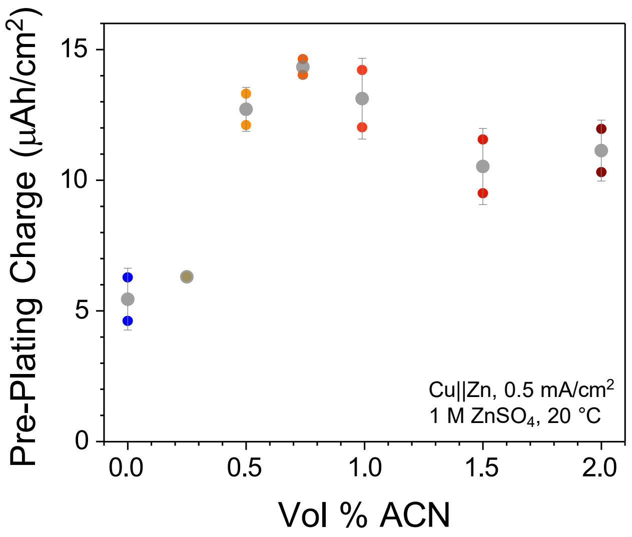

Stefan Ilic, Michael J. Counihan, Sydney N. Lavan, Yingjie Yang, Yinke Jiang, Diwash Dhakal, Julian Mars, Emma N. Antonio, Luis Kitsu Iglesias, Timothy T. Fister, Yong Zhang, Edward J. Maginn, Michael F. Toney, Robert F. Klie, Justin G. Connell, and Sanja Tepavcevic *Effect of Antisolvent Additives in Aqueous Zinc Sulfate Electrolytes for Zinc Metal Anodes: The Case of Acetonitrile, ACS Energy Letters* 2024 *9* (1), 201-208. doi: 10.1021/acsenergylett.3c02504

Counihan, M. J., Roberts, L., Ilic, S., Yang, Y., Ely, C., Klie, R. F., Toney, M. F., & Tepavcevic, S. *How does an antisolvent additive affect all interfaces in aqueous Zn–MnO2 batteries?*. Journal of Materials Chemistry A, 13(23), 17730-17739. (2025). doi:10.1039/D5TA00951K.

Neelam Omprakash Sunariwal, Thanh Le, Xiaoran Yang, Trenton Gallagher, Jordi Cabana, Tim Vosburgh and Sanja Tepavcevic *Effect of Pre-Conditioning on Cycling Performance of Aqueous Zn-Ion Batteries* (submitted)

GALVANOSTATIC CYCLING OF A Cu/Zn HALF CELL: 1ST CYCLE

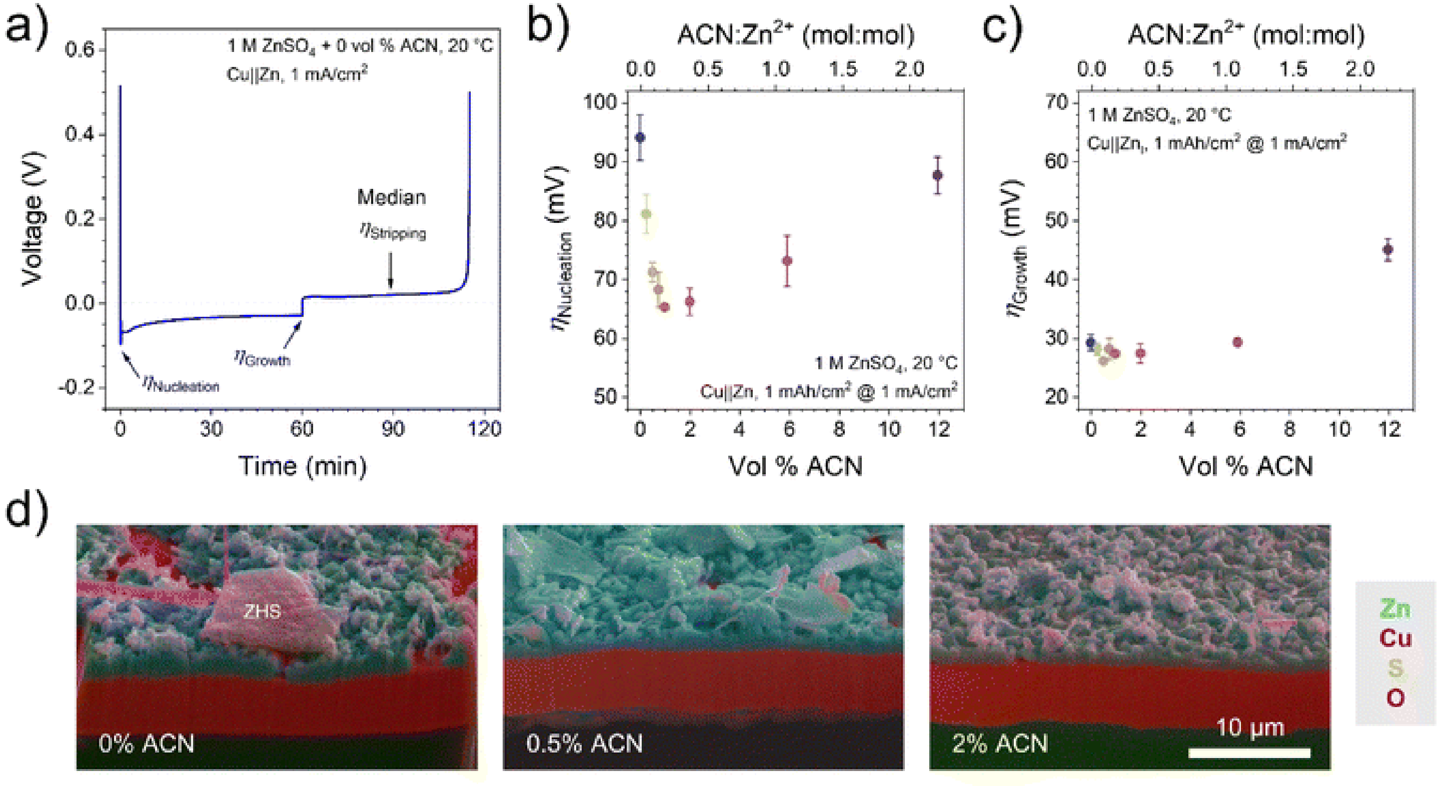

- **There is a local minimum in both Zn nucleation and growth overpotentials in the 0.5–2 vol% ACN range before greater ACN concentration increases the overpotentials above low-ACN concentration.**
- SEM-EDX cross-section images of plated Zn on Cu electrodes after 100 plating/stripping steps show that even 0.5% ACN drastically changes ZHS distribution within plated Zn, while Zn morphology still similar after many cycles regardless of ACN

CUMULATIVE COULOMBIC EFFICIENCY (CCE) OVER 100 CYCLES FOR Cu||Zn CELLS

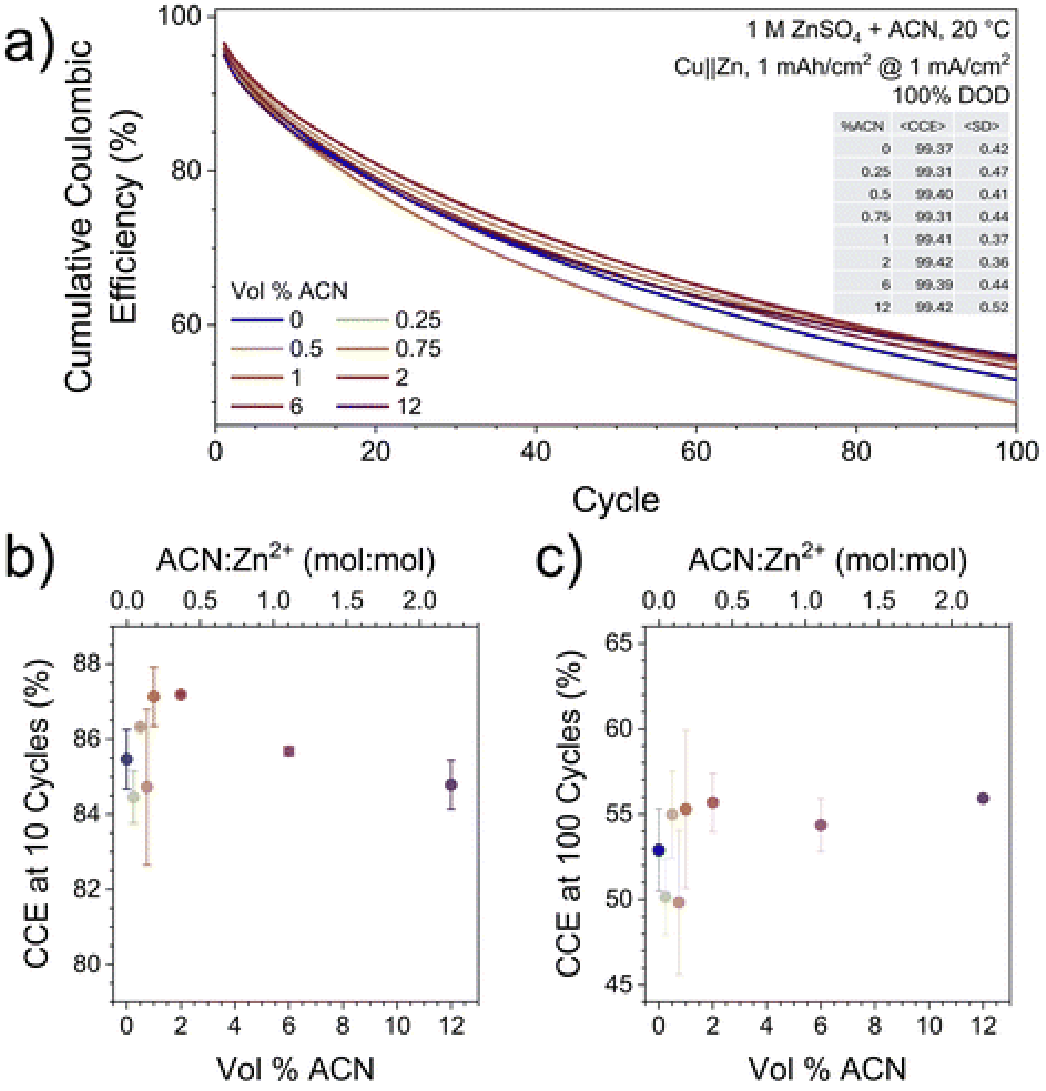

%ACN	<CCE>	<SD>
0	99.37	0.42
0.25	99.31	0.47
0.5	99.40	0.41
0.75	99.31	0.44
1	99.41	0.37
2	99.42	0.36
6	99.39	0.44
12	99.42	0.52

$$\text{Cumulative CE} = 100 \times \prod_{1}^{n} \frac{Q_{\text{strip},n}}{Q_{\text{plate},n}}$$

- Cumulative Coulombic Efficiency measures charge loss in the cell by integrating the efficiency over every cycle
- Zn loss can occur *via* dead Zn formation or through corrosion (which leads to ZHS formation).
- After 10 cycles the CCE is maximized at 0.5–2 vol% ACN, in line with the optimized overpotentials
- After 100 cycles, however, the only trend is that adding any ACN concentration generally improves CCE above the pure aqueous electrolyte

XRD PATTERN OF A CU ELECTRODE AFTER 1 AND 100 PLATE/STRIP CYCLES

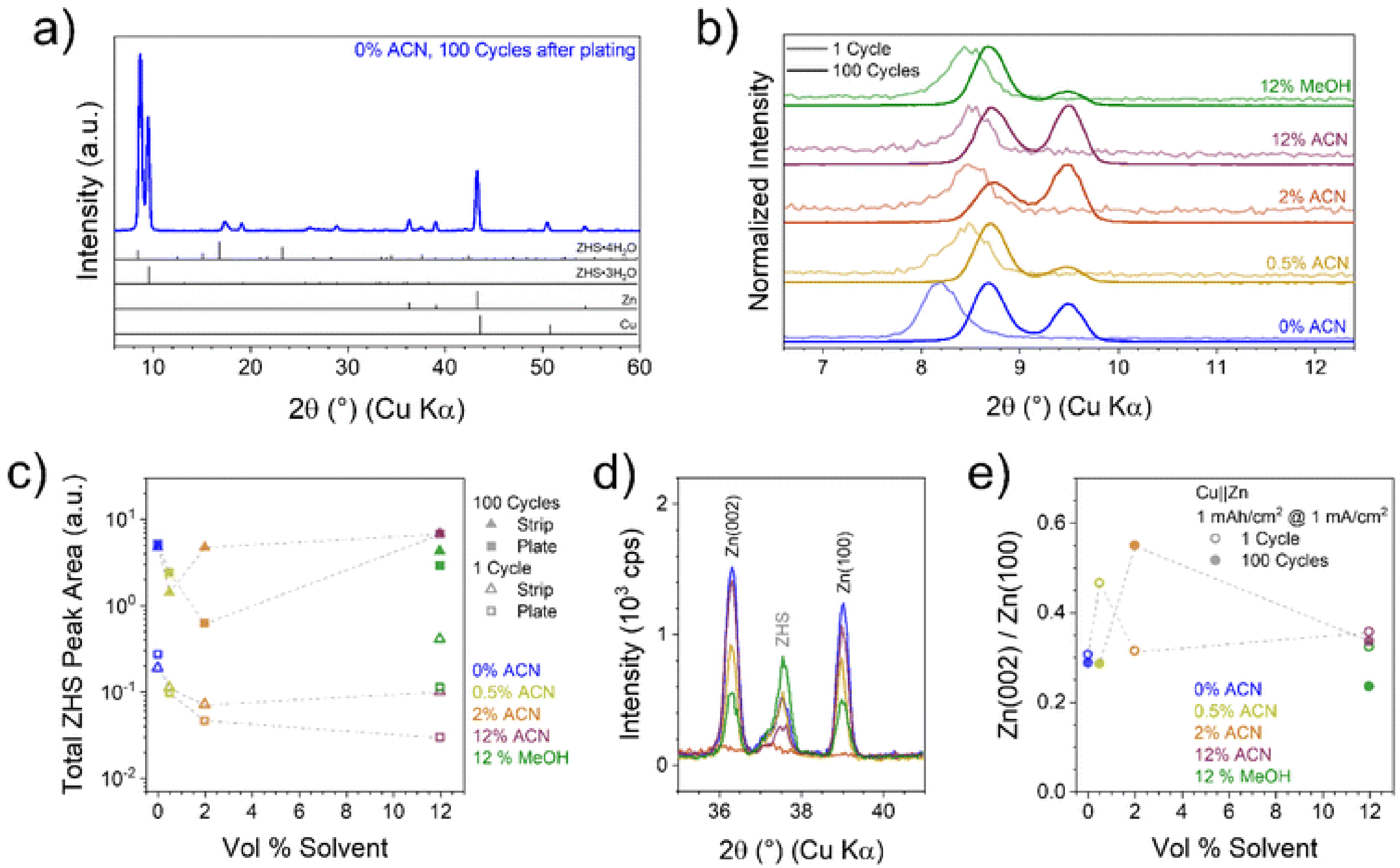

- ZHS structure affects interfacial ion transport and/or local pH changes
- Most dependent on antisolvent additions during the initial cycling stages.
- Clear differences in the ZHS amount and structure showing antisolvent strength, H-bonding can influence ZHS growth
- Low amounts of ACN (0.5–2 vol%) shift the texturing towards more Zn(002) after the first plating step and after 100 cycles
- **Aligns with lower plating overpotentials and lower amounts of ZHS, indicating 0.5–2 vol% is the optimal ACN concentration for Zn anodes.**

GALVANOSTATIC CHARGE–DISCHARGE CURVES OF Zn‖delta-MnO$_2$ FULL CELLS

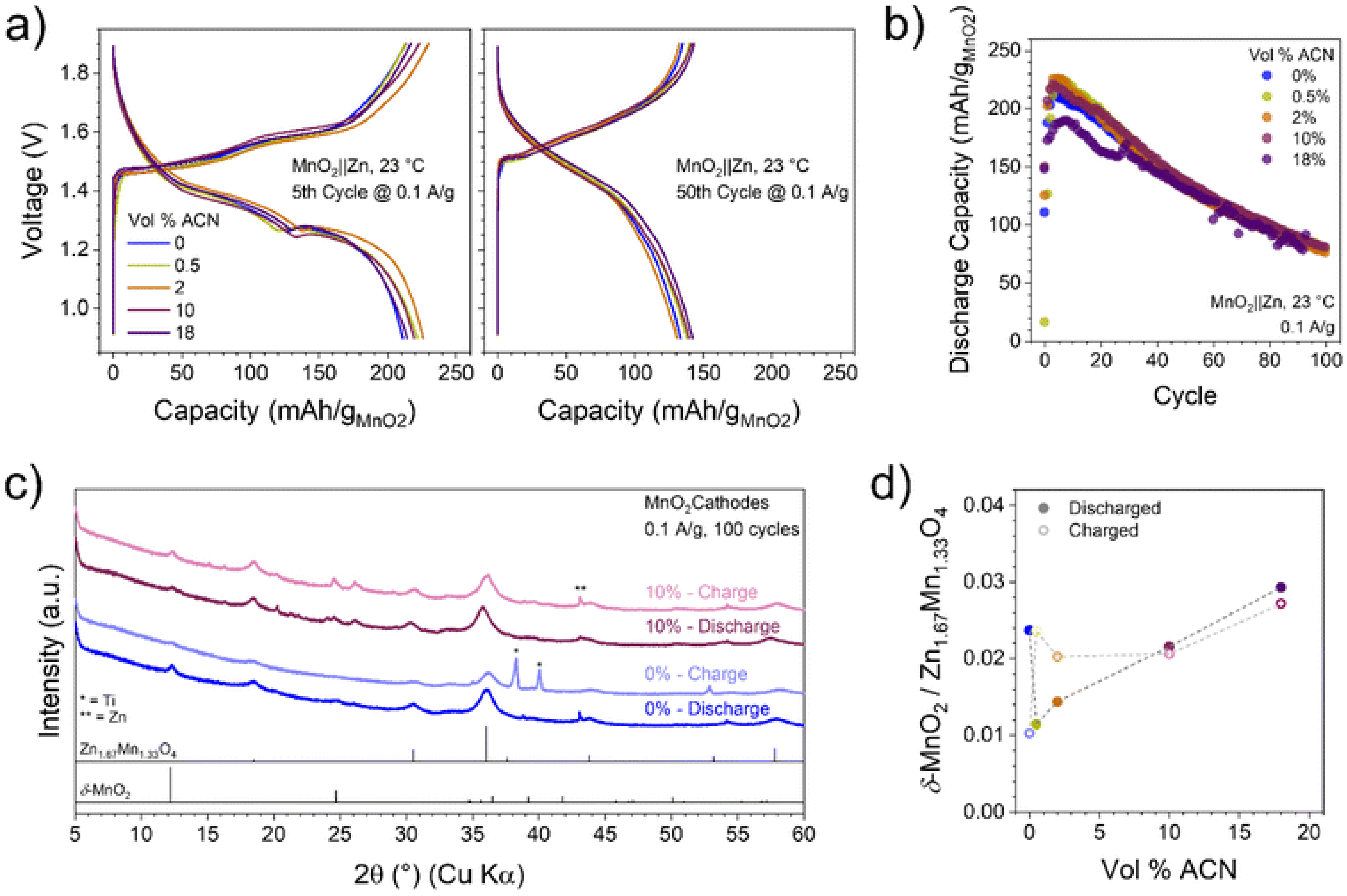

- Voltage profiles same in shape and capacity over time indicating ACN may have much less impact on the cathode than the anode.
- δ-MnO$_2$ content in discharged cells increases with ACN concentration, suggesting that acetonitrile slows or partially suppresses the transformation to Zn$_{1.67}$Mn$_{1.33}$O$_4$ during cycling.
- **ACN modulates the phase evolution, but it does not eliminate the primary degradation mechanism.**

Zn‖MnO$_2$ FULL CELL AT OPEN CIRCUIT VOLTAGE

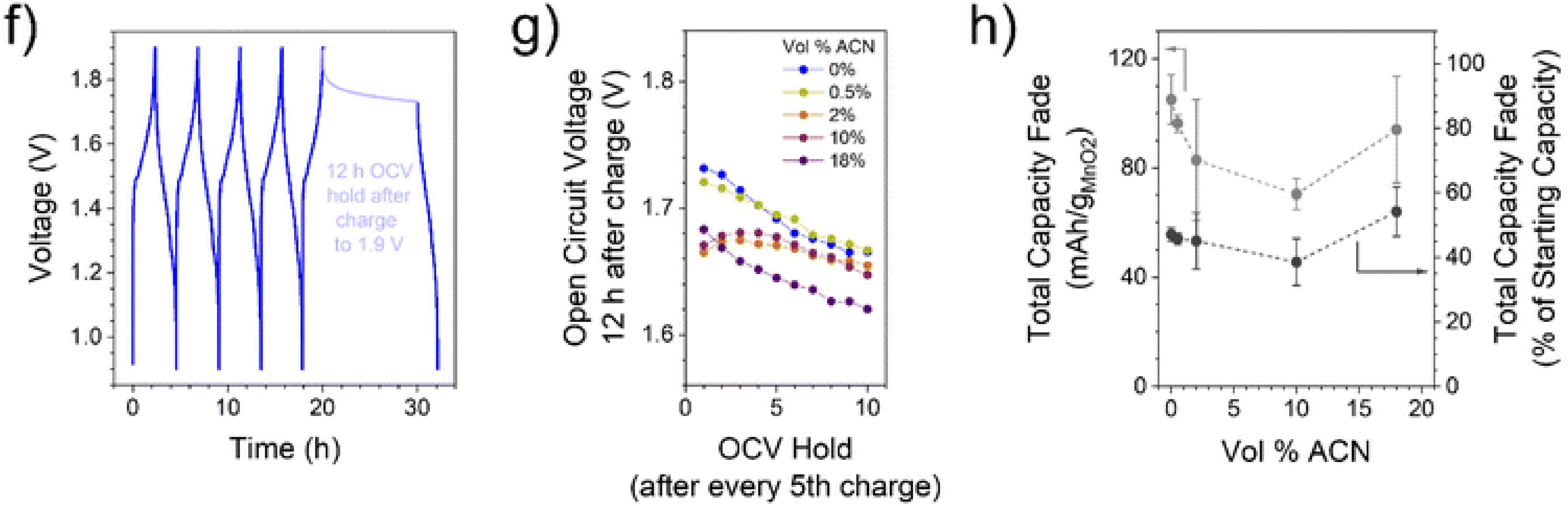

- Simulated rest periods (calendar aging) that a practical battery would experience
- Example voltage profiles showing charge–discharge cycles with a 12 h open circuit rest period after every fifth charge cycle at 0.1 A g_{MnO2}^{-1}.
- Open circuit voltage at the end of the rest period over 50 cycles (10 total rest periods).
- 2 and 10 vol% ACN show minimal losses over the same time (<50 mV).

Stefan Ilic, Michael J. Counihan, Sydney N. Lavan, Yingjie Yang, Yinke Jiang, Diwash Dhakal, Julian Mars, Emma N. Antonio, Luis Kitsu Iglesias, Timothy T. Fister, Yong Zhang, Edward J. Maginn, Michael F. Toney, Robert F. Klie, Justin G. Connell, and Sanja Tepavcevic *Effect of Antisolvent Additives in Aqueous Zinc Sulfate Electrolytes for Zinc Metal Anodes: The Case of Acetonitrile, ACS Energy Letters* 2024 *9* (1), 201-208. doi: 10.1021/acsenergylett.3c02504

Counihan, M. J., Roberts, L., Ilic, S., Yang, Y., Ely, C., Klie, R. F., Toney, M. F., & Tepavcevic, S. How does an antisolvent additive affect all interfaces in aqueous Zn–MnO2 batteries?. Journal of Materials Chemistry A, 13(23), 17730-17739. (2025). doi:10.1039/D5TA00951K.

Neelam Omprakash Sunariwal, Thanh Le, Xiaoran Yang, Trenton Gallagher, Jordi Cabana, Tim Vosburgh and Sanja Tepavcevic *Effect of Pre-Conditioning on Cycling Performance of Aqueous Zn-Ion Batteries* (submitted)

MNO$_2$ BALL-MILLED AND COATED ON STAINLESS STEEL FOIL

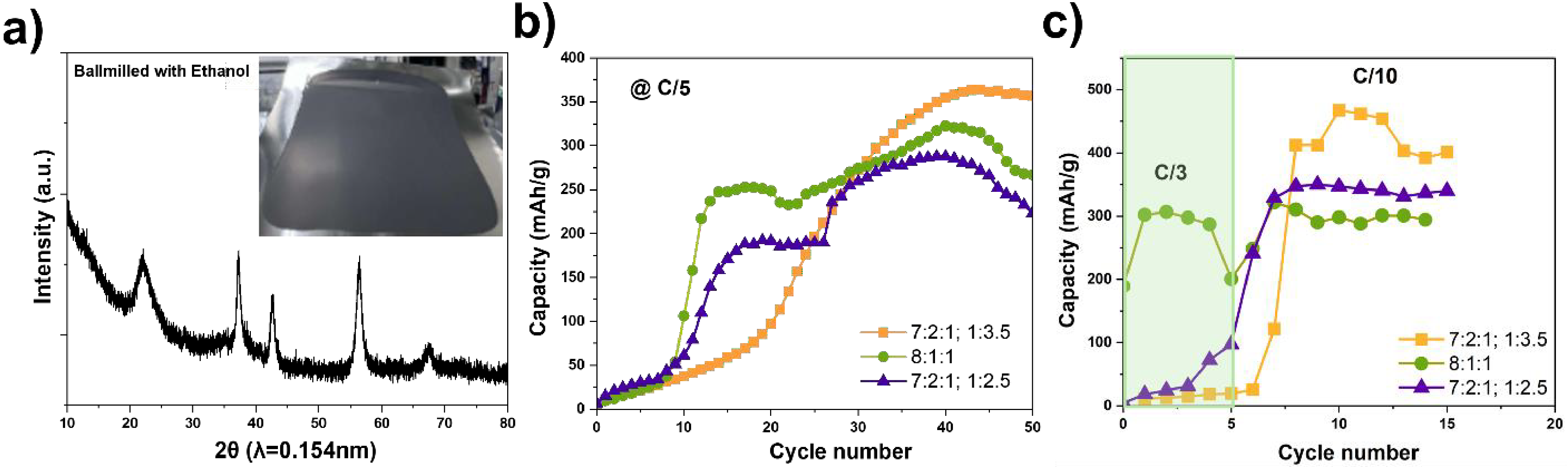

- Ball milled electrodes showed improved wetting and higher capacity vs. non-ball milled.
- The ratio of active material, conductive carbon, and binder influenced the cycling stability and maximum discharge capacity achieved.
- The 7:2:1 ratio with high solvent to solid ratio of 1:3.5 shows the highest capacity of over 360 mAh/g at C/5
- Slow-to- Fast Rate Cycling at RT did not significantly improve capacity

FAST-TO-SLOW PRECONDITIONING AND RATE CYCLING AT RT

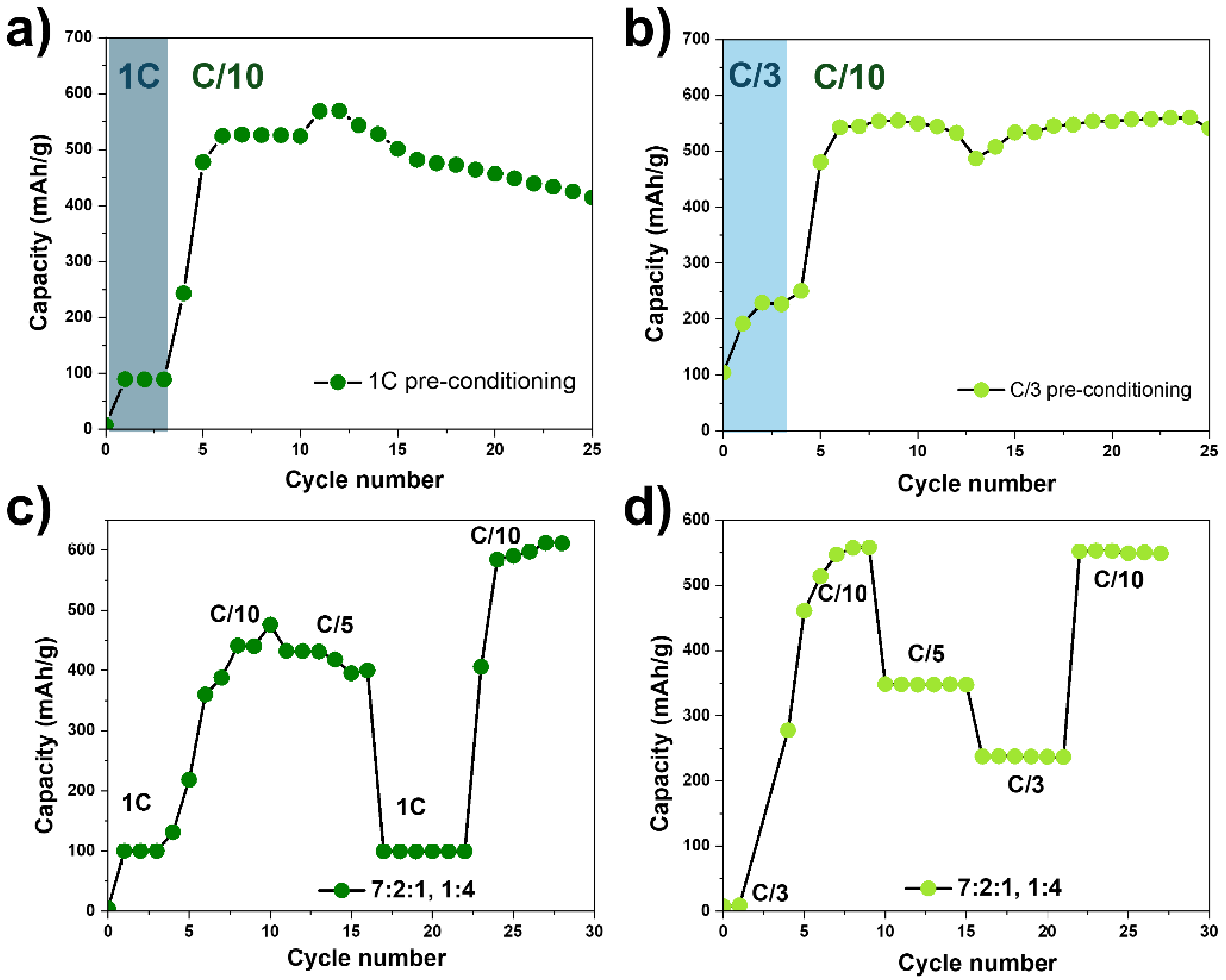

- **Fast-to-slow formation cycling preconditioning at RT** gave the largest sustainable capacity improvements (~500–550 mAh/g)
- **Fast-to-Slow formation cycling preconditioning at 50°C**
  - Continuous high-T cycling gave the highest peak capacity (~600 mAh/g) but at the cost of rapid degradation.
- **Fast-to-Slow Rate Cycling at Room Temperature**
  - Faster preconditioning improved active material utilization.
  - Impedance decreased after the initial fast cycles, indicating better electrode/electrolyte interface formation.

EFFECT OF CATHODE LOADING ON CAPACITY RETENTION

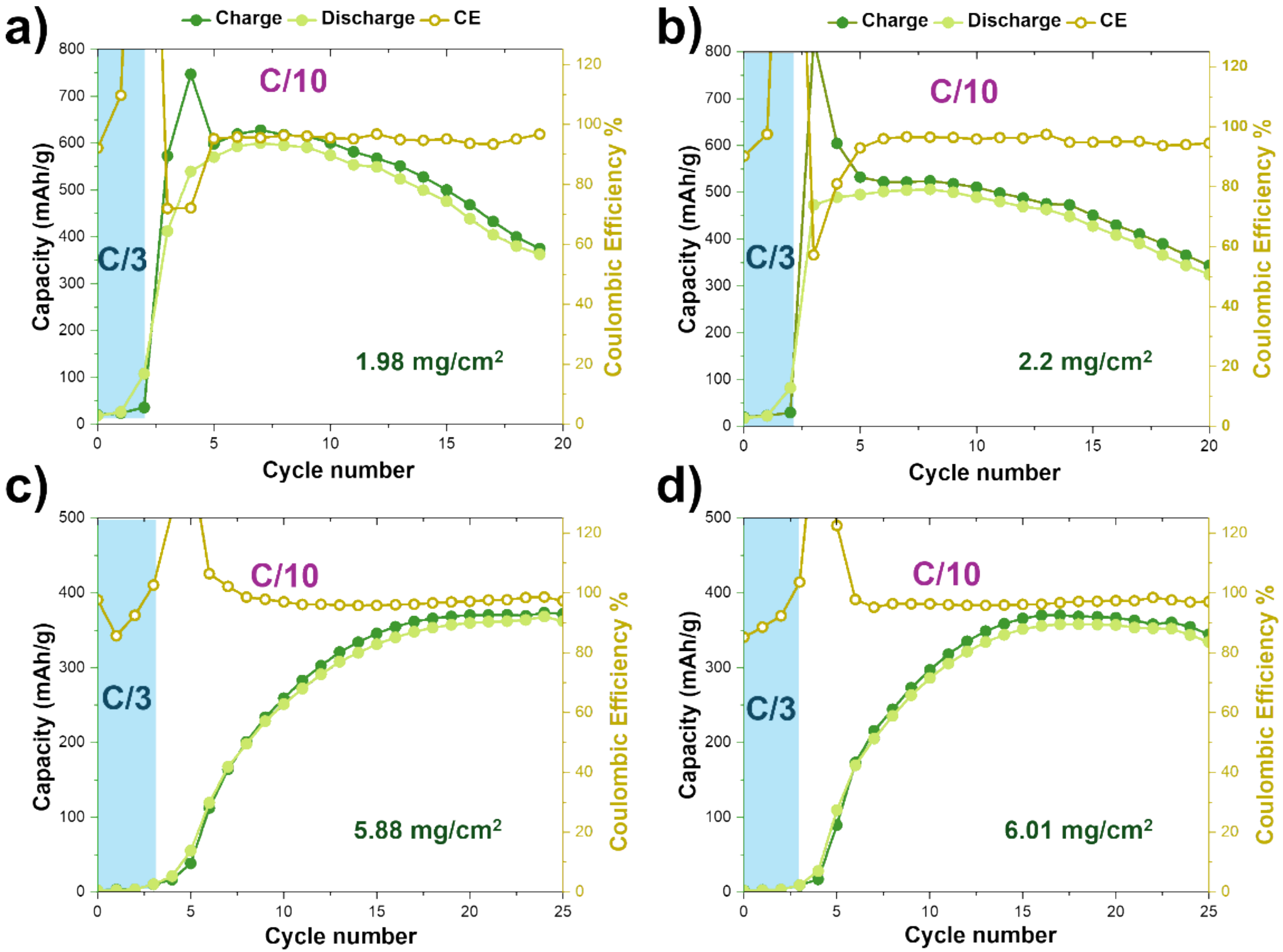

- Different loading of ball-milled MnO$_2$ active material coated on 304 stainless steel foil and assembled into coin cells at Coulomb Technology

- Fast-to-slow formation cycling preconditioning at RT:
  - 3 cycles at C/3 followed by C/10 cycling

- MnO2 loading ~2mg/cm^2: achieved capacity of ~500–600 mAh/g

- MnO2 loading ~6mg/cm^2 : achieved capacity of ~350 mAh/g

Cycling Induced Phase Transformations of EMD

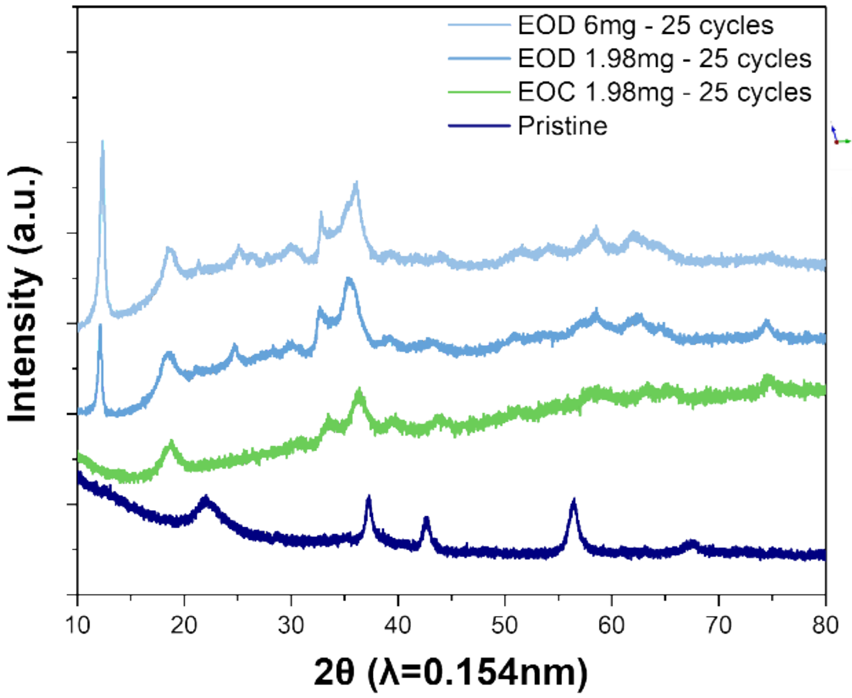

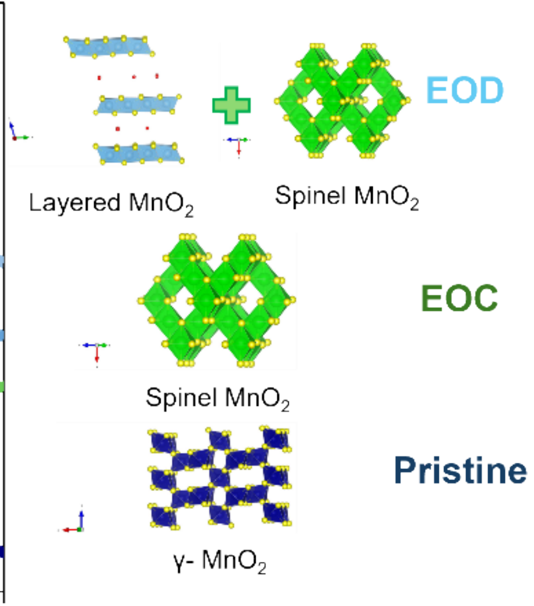

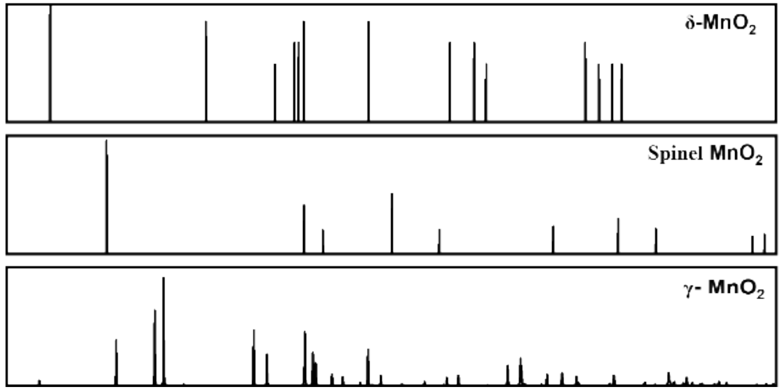

JCPDS# 42-1317

JCPDS# 24-1133

JCPDS# 14-0644

- Powder XRD after 25 cycles for end of charge (EOC), end of discharge (EOD) with low and high loading cathode
- Initial γ-phase of MnO_2 after 25 cycles turns into $ZnMn_2O_4$ type spinel phase.
- At EOD, new peaks arose at low 2θ around 12° and around 25° appeared, which were ascribed to a layered δ-phase.
- With low loading cathode thickness ~27µm and high loading ~55µm, no obvious differences were observed between the cycled cathodes after 25 cycles due to limitation of Cu Kα X-ray source,
- Desing approaches to preserve layered, d-MnO_2 polymorph formed after initial fast rate pre-conditioning to retain high specific capacities over long term cycling.

CONCLUSIONS

Antisolvent effects at anode and cathode interfaces

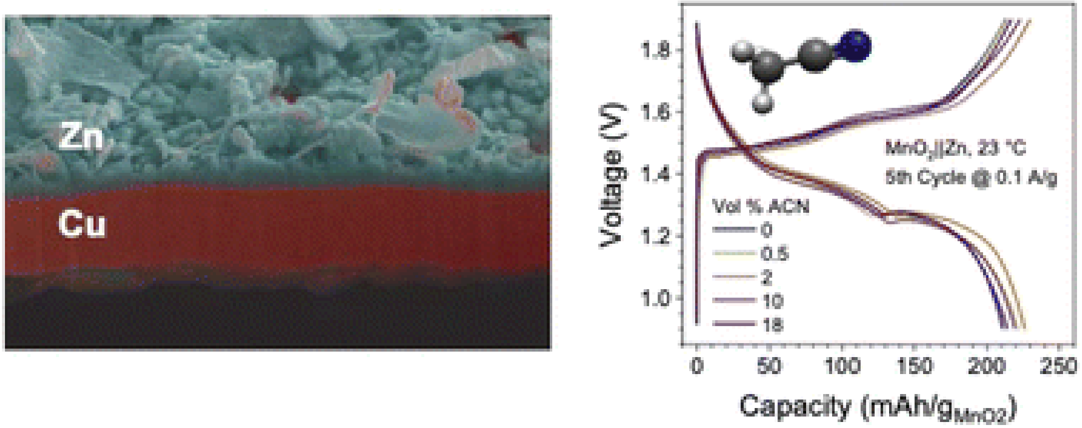

- Acetonitrile addition to $ZnSO_4$ electrolyte leads to antisolvent behavior: it is excluded from the Zn^{2+} and SO_4^{2-} solvation shells in the bulk electrolyte but adsorbs on the electrode surface and changes interfacial solvation structures.
- This leads to improved zinc metal plating morphologies and lower HER rates, which cumulatively increase the efficiency of Zn plating and stripping.
- Low (0.5–2 vol%) ACN concentrations showed local minima for Zn plating and stripping overpotentials and highest cumulative CE efficiency over 100 cycles in both half-cell (Cu/Zn) and full cell (MnO2/Zn) configurations
- Ball milling of MnO_2 and coating on stainless steel foil show positive impact on specific capacity.
- Short high-temperature preconditioning and/or fast-to-slow formation cycling achieved the largest capacity improvements (~500–600 mAh/g) for the low loading of active material (~2mg/cm^2).
- Controlling extensive phase transformations during electrochemical cycling of MnO_2 cathodes with approaches to preserve layered, d-MnO_2 polymorph can retain high specific capacities over long term cycling

ACKNOWLEDGEMENTS

Dr. Michael Counihan (ANL)

Dr. Stefan Ilic (ANL)

Dr. Sydney Lavan (ANL)

Dr. Yingjie Yang (UIC)

Diwash Dhakal (ANL)

Dr. Julian Mars (CU Boulder)

Dr. Emma Antonio (CU Boulder)

Lacey Roberts (CU Boulder)

Yinke Jiang (ND) – Computation

Dr Toru Hatsukade (ANL)

Dr. Justin Connell (ANL)

Dr Nigel N. Becknell (ANL)

Pietro Papa Lopes (ANL)

Prof. Robert Klie (UIC)

Dr. Timothy Fister (ANL)

Prof. Michael Toney (CU Boulder)

Prof. Yong Zhang (ND)

Neelam Omprakash Sunariwal (UIC)

Thanh Le (Coulomb Technology)

Xiaoran Yang (Coulomb Technology)

Trenton Gallagher (Coulomb Technology)

Jordi Cabana (UIC & ANL)

Tim Vosburgh (Coulomb Technology)

JCESR JOINT CENTER FOR ENERGY STORAGE RESEARCH

cradle to commerce

coulomb TECHNOLOGY

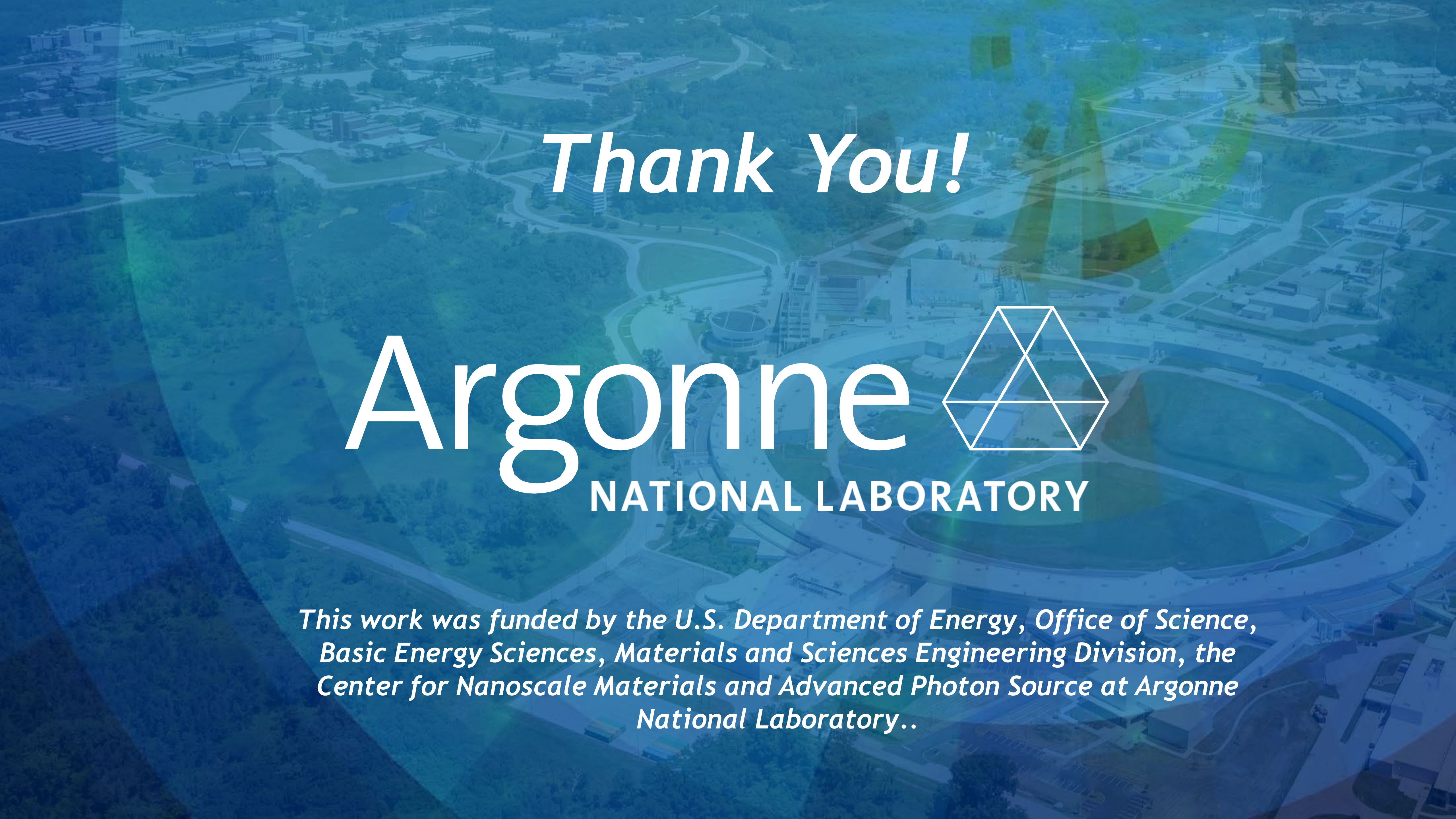

Thank You!

Argonne
NATIONAL LABORATORY

This work was funded by the U.S. Department of Energy, Office of Science, Basic Energy Sciences, Materials and Sciences Engineering Division, the Center for Nanoscale Materials and Advanced Photon Source at Argonne National Laboratory..

BERKELEY LAB

BEYOND LITHIUM ION XVI

BEYOND Lithium Ion XVI

Lawrence Berkeley National Laboratory

Bay Area, CA I JUNE 23-25, 2026

The **16th Beyond Lithium-Ion Conference (BLI-XVI)** will be hosted by LBNL in bay area, CA from **June 23 to June 25, 2026.** This meeting continues a series of symposia organized by a consortium of U.S. National Laboratories (ANL, LBNL, LLNL, NREL, ORNL, PNNL, and SLAC), IBM and NASA Research Centers to bring together scientists and engineers, focusing on advances in scalable energy storage beyond the current state-of-the-art lithium-ion batteries.

Argonne NATIONAL LABORATORY

Lawrence Livermore National Laboratory

NREL NATIONAL RENEWABLE ENERGY LABORATORY

OAK RIDGE National Laboratory

Pacific Northwest NATIONAL LABORATORY

SLAC NATIONAL ACCELERATOR LABORATORY

IBM®

NASA